ELSEVIER

Surface Science 469 (2000) 55–64

surface science

www.elsevier.nl/locate/susc

Three-dimensional view of the thermal desorption reaction: copper on rhenium(0001)

R. Wagner, K. Christmann *

Institut für Chemie der Freien Universität, Bereich Physikalische und Theoretische Chemie, Takustraße 3, D-14195 Berlin, Germany

Received 21 January 2000; accepted for publication 25 July 2000

Abstract

The application of the Polanyi–Wigner equation to describe the rate R_{des} of a thermal desorption process from a homogeneous surface is common practice in surface science temperature-programmed desorption (TPD) studies. Current evaluation methods (known as line-shape analyses) deduce from series of thermal desorption traces [coverage (Θ)-dependent] energetic and kinetic parameters such as desorption energy, desorption order or frequency factor. The TPD spectra themselves, i.e., the function $R_{des}(T)$, as well as the output of such an analysis (e.g., the remaining coverage Θ_{res} as a function of T for a given initial coverage), represent parametrized two-dimensional (2D) graphs. It will be shown in this work by means of selected examples [taken from noble metal desorption from a Re(0001) surface] that the 2D graphs are nothing but projections of R_{des} on to either a rate–temperature or a rate–coverage plane. By using the three-dimensional (3D) representation of R_{des} in T, Θ space, valuable information on phase transitions occurring during the desorption process, on multiple TPD states and interlayer interactions can easily be visualized and exploited.

Keywords: Copper; Rhenium; Thermal desorption spectroscopy

1. Introduction

Thermal desorption spectroscopy (TDS) [also often named temperature-programmed thermal desorption (TPD)] is a fairly simple (regarding instrumentation) but quite powerful experimental technique to determine the energetic and kinetic as well as the structural properties of particles adsorbed on solid surfaces. Accordingly, a vast amount of literature has been accumulated over the past 50 years and we refer only to few especially helpful and revealing review articles [1–12]. The physical properties of interest that can principally be extracted from a series of TPD spectra or even from a single TPD trace concern adsorption energies, particle–particle interaction energies, desorption orders, pre-exponential factors and the respective coverage dependencies, (relative) particle coverages, and in suitable cases also absolute particle numbers (coverages). Furthermore, conclusions can be drawn on the growth behavior especially of metallic deposits, growth kinetics, etc. [13].

In the 1960s and 1970s in particular various methods and procedures were developed to extract all these types of information from TPD spectra, and we refer to a few particularly revealing reviews [8,14]. Another promising way of getting access

* Corresponding author. Fax: +49-30-8385-4792.
E-mail address: kchr@chemie.fu-berlin.de (K. Christmann)

0039-6028/00/$ - see front matter
PII: S0039-6028(00)00771-8

to the system's properties is to simulate the experimental TPD spectra by model calculations taking into account and optimizing suitable parameters to fit the experimental thernal desorption (TD) traces. Again, we cite some essential papers in the field [15–19]. Most of the aforementioned methods and procedures represent per se comfortable and powerful tools to obtain the desired physical information, provided they are applied carefully to reliable experimental data. However, they are quite different as regards the kind of representation but also the applied mathematical approximation required for the data evaluation. The present paper attempts to provide a physical connection between these various methods and to supply the reader with an interesting and quite helpful novel graphical representation of TPD data which has become possible relatively easily by using modern personal computers. This will be demonstrated with the help of recent experimental data that were obtained with metal-on-metal desorption (copper from rhenium) in our laboratory. More details about this adsorption system can be found in the original work [20,21].

2. The desorption experiment

The main advantage of the TPD experiment consists of its simplicity, and yet it provides — if it is performed appropriately — valuable information on the energetics and kinetics of an adsorption system. The crucial quantity is the temperature of the system which is (mostly in a linear fashion) ramped by supply with a certain amount of thermal energy. The sample, which is covered with a well-defined amount of adsorbate particles prior to the application of the temperature program, is then moved in front of the ionization source of a mass spectrometer until the thermal energy (mostly electrically) is supplied to the sample. In many TPD experiments, this sample consists of a metal single crystal (area approximately 1 cm^2, thickness 1 mm) provided with an appropriate thermocouple to control the temperature. The property being measured in most cases is the rate of desorption, expressed as the temperature derivative of the coverage: $R_{des} = d\Theta/dT$, whereby a linear temperature ramp is tacitly assumed:

$$T = T_0 + \beta t, \tag{1}$$

with heating rate $\beta = dT/dt = \text{constant}$.

In a pumped vacuum system, R_{des} is linearly correlated with the signal intensity of the mass spectrometer tuned to the respective partial pressure of the adsorbate. This kind of measurement is of two-dimensional character; i.e., the rate R_{des} is followed as a function of temperature T for several (increasing) initial coverages Θ_0. As a result, one obtains the typical thermal desorption spectrum, and an example is given in Fig. 1 taken from our data for copper desorbing from a Re(0001) surface [20,21]. However, the initial 'state' of the system is not completely characterized by the temperature, for the second decisive quantity is the (momentary) adsorbate coverage Θ_{res}: as the TPD experiment proceeds in time (or temperature) Θ_{res} decreases and finally vanishes as the desorption is complete, i.e., all adsorbate particles have left the surface. Although Θ_{res} is not explicitly followed in the standard TPD experiment, it can be determined later as a relative quantity, by considering that

$$R_{des} = -\frac{d\Theta}{dT} = -\frac{\dot{\Theta}}{\beta}. \tag{2}$$

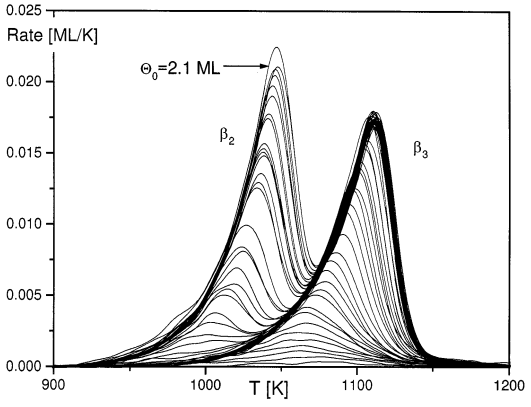

Fig. 1. Family of copper thermal desorption spectra obtained from a Re(0001) surface with a heating rate of 7.7 K s^{-1}. The copper deposition was performed at 673 K up to a coverage of 2.1 monolayers (ML). Parameter of the curves is the initial coverage. Clearly, the first and second monolayer states (β_3 and β_2) can be distinguished.

By numerically integrating the values of the desorption rate beginning from the high-temperature side to the momentary temperature T_i, i.e., opposite to the direction of the temperature ramp, one can obtain the corresponding momentary coverage Θ_i and, hence, pairs of values for Θ_i and T_i (N_{ML} is a normalization constant):

$$N_{ML}\int_{T_i}^{T_{max}} |-\beta R_i|\,dT=\Theta_i(T). \quad (3)$$

In this way, one can easily obtain the temperature-dependent residual coverage $\Theta_{res}(T)$ with the initial coverage Θ_0 being a parameter, and this function is reproduced in Fig. 2, based on the TPD data presented before in Fig. 1. Often the Θ_{res} and T axes are inverted, which has the advantage that the TPD peaks can easily be associated with a certain coverage (β states in Figs. 1 and 2). In principle, the curves of Fig. 2 characterize the behavior of the desorption system for this desorption process completely. They are trajectories in the 'plane of state' of the system. The function $T(\Theta_{res})$ allows information to be drawn about the interactions between different adsorbed layers [15]. Furthermore, they can reveal phase boundaries and phase transitions of the desorbing system [22]. Actually, we have seen that the process of thermal desorption is a three-dimensional one; in other words, the experimentally measured rate of desorption is a quantity that depends on two variables: coverage Θ and temperature T. This can be made clear by the generalized Polanyi–Wigner equation [23]:

$$R_{des}(\Theta, T)=\frac{\nu(\Theta, T)}{\beta}\,\Theta^n \exp\left(-\frac{Q_{des}(\Theta, T)}{RT}\right), \quad (4)$$

in which $\nu(\Theta, T)$ means the coverage- and temperature-dependent frequency factor (pre-exponential), n the reaction order, and $Q_{des}(\Theta, T)$ the heat of desorption (desorption energy). For simplicity, we have used the symbol Θ instead of Θ_{res} in this equation and will tacitly use the symbol Θ throughout the following text, since it refers to the actual surface coverage for which Eq. (4) holds.

Eq. (4) is a fairly general equation, it only requires a homogeneous adsorption system in which a single desorbing species occupies identical and equivalent surface sites. It holds equally well for the evaporation process of a homogeneous material (surface and desorbing species are chemically identical) — in this case $|Q_{des}|$ equals the sublimation enthalpy and ν describes the perpendicular vibration of the adatom against the substrate (ν is normally assumed to be the universal frequency factor, i.e., equal to $kT/h=6\times10^{12}$ s^{-1}) — or it may describe the desorption from thick multilayers of a condensed adsorbate on a substrate of a different material (in this case, desorption energy and pre-exponential are independent of coverage and temperature). A somewhat different situation is encountered if we consider the desorption of thin (noble) metal films from refractory metal surfaces (molybdenum, tungsten, rhenium). Here, we refer to our aforementioned example of copper desorbing from a Re(0001) surface [21]. In this particular case, both the desorption energy and the pre-exponential depend on both coverage and temperature, and even the reaction order may vary with T and Θ: $n(\Theta, T)$.

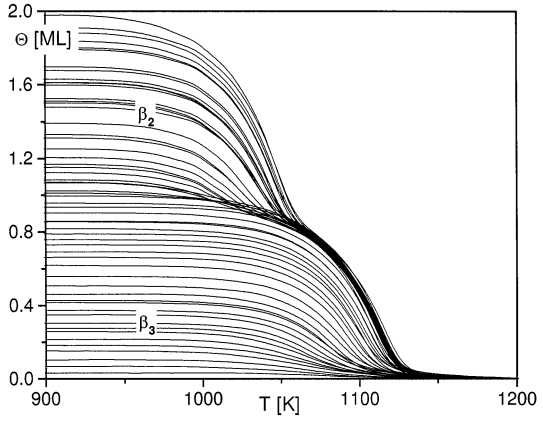

Fig. 2. Plot of the residual copper coverage Θ_{res} (in monolayers) as a function of temperature T, for different initial coverages Θ_0 up to two monolayers. The two desorptions states β_3 and β_2 are indicated.

3. The desorption trajectories

We recall that the graph $R_{des}(\Theta, T)$ is equivalent to a complete and unambiguous representation of

the desorption process, and this graph is obtained by numerically integrating the desorption rate for successively increasing sample temperature as described above; each point in this graph is characterized by a triple of values: Θ_i, T_i and $R_{\mathrm{des},i}$. In other words, any desorption rate $R_{\mathrm{des},i}$ is a function of the two state variables: (momentary) coverage Θ_i and (momentary) temperature T_i. This implies a three-dimensional (3D) representation of this function, and we have constructed the respective plot in Fig. 3 using the thermal desorption spectra of Fig. 1 for the copper desorption from Re(0001). One can actually see that the 'two-dimensional' TD spectra with their different initial coverages are 'transformed' to desorption 'trajectories' which describe the evolution of the desorption in the three-dimensional parameter space. The individual desorption states are well separated and can be viewed at from different angles. The trajectories can be projected either in the coverage (temperature) plane (=base plane of the cube), or in the rate (temperature) 'plane of state' (=right plane in the rear, →'normal' TPD spectra), or, finally, in the rate (coverage) plane (=left plane in the rear, →'layer plots', see below). All three kinds of these projections are also reproduced in Fig. 3.

In order to underline the advantage of this 3D representation we just consider the normal TPD spectra, i.e., the projection of R_{des} in the temperature plane. When looking at the respective two-dimensional (2D) graph, no real information of the coverage is obtained except the (trivial) fact that Θ decreases with increasing temperature. Fig. 3, however, allows a much more detailed insight into the development of the coverage with increasing temperature. Due to the exponential character of the Polanyi–Wigner equation [Eq. (3)] the coverage dependence can be more easily rationalized if this equation is written in a logarithmic form [24,25]:

$$\ln R = \ln \frac{\nu}{\beta} + n \ln \Theta + \frac{Q_{\mathrm{des}}}{RT}. \tag{5}$$

For a given coverage Θ this relation reflects, among others, the inverse temperature dependence of the logarithm of the desorption rate, which is plotted in Fig. 4 again based on the TPD spectra of Fig. 1.

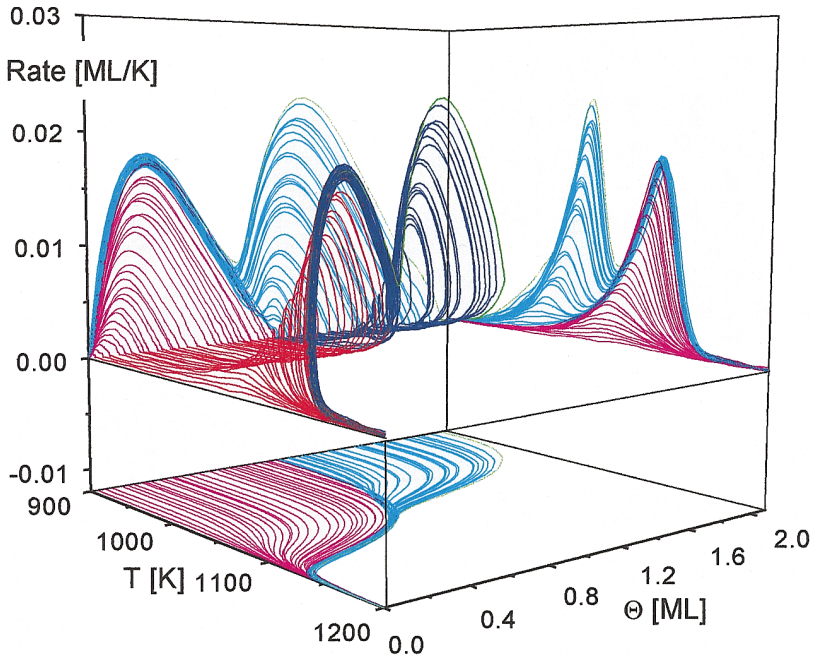

Fig. 3. Three-dimensional representation of the functional dependence of the desorption rate R_{des} on coverage and temperature. Also shown are the projections of this function on to the coverage and temperature plane, respectively.

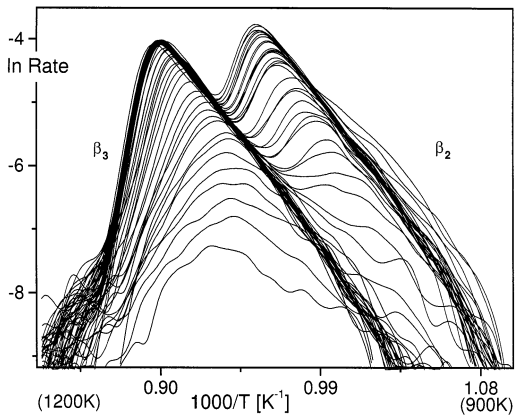

Fig. 4. Plot of the logarithm of the desorption rate against the reciprocal temperature, for the copper desorption spectra of Fig. 1. See text for more details.

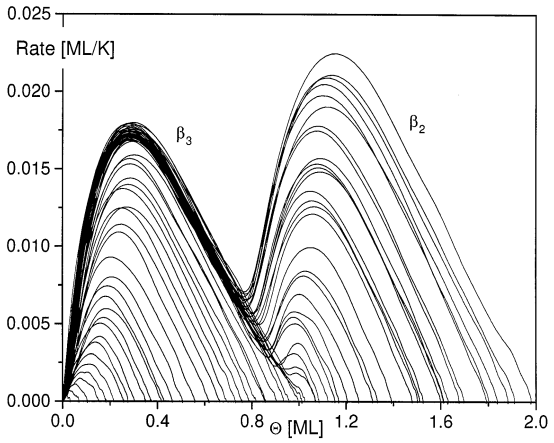

Fig. 5. Layer plots for the TD spectra displayed in Fig. 1. Parameter of the curves is the intial coverage, Θ_0. Note that the temperature (which is an implicit parameter here) rises from right to left! The two desorption states β_3 and β_2 are clearly recognizable.

As long as the reaction order n is zero and Q_{des} and ν remain constant, all trajectories of a given TD state should form straight lines with positive slope; they simply reflect the genuine exponential increase of the desorption rate with temperature. In Fig. 4, this is apparently fulfilled for certain (small) temperature ranges for both the β_2 and the β_1 desorption states (which have their leading edge in different T intervals). In these linear ranges it is quite straightforward to evaluate the respective Arrhenius parameters according to Eq. (5) (procedure by Polanyi). One can circumvent the condition of constant n, Q_{des} and ν by constraining the evaluation procedure to a very small range of desorption (in which any changes of the parameters do not play a significant role). This method is known as 'threshold analysis' and has been developed successfully applied by Habenschaden and Küppers [12].

If we look at the projection of the 3D rate function on to the rate–coverage plane the already mentioned 'layer plots' are obtained, which were first introduced by Schlichting and Menzel [24]. Note that in these layer plots the desorption occurs from right to left, i.e., in the reverse direction to which 'normal' TPD spectra are viewed. A typical set of layer plots is shown as Fig. 5, in which the desorption rate R_{des} (ML K^{-1}) is plotted against the coverage Θ (ML). Several features of these layer plots are noteworthy. In a fairly large initial coverage range both in the first ($0.9>\Theta>0.3$) and second ($2.0>\Theta>1.2$) monolayer, the individual curves exhibit — depending, of course, on the initial coverage — a practically linear range (with negative slope) which is, according to Schlicting and Menzel [24], characteristic for a desorption order of zero. At first glance it may be difficult to understand this constant slope with Θ, since, with $n=0$ and constant Arrhenius parameters, Eq. (4) does not contain an apparent linear relationship with Θ. However, again the 3D representation of Fig. 3 is helpful here. It reveals that the linear character is indeed caused by the common temperature variation in this range. All in all, the layer plots have the advantage that they clearly show peaks separated by a (more or less sharp) minimum that can easily be associated with the formation of individual layers (e.g., during growth of metal on metals) or at least desorption binding states.

Actually, the rate of desorption is not the only quantity which can be used to describe and characterize the desorption system. Equally suited are, for example, the chemical potential μ [22,26], the heat of desorption [22], or the mean lifetime of a particle τ, which was first introduced as a temperature- and coverage-dependent quantity by Bauer and co-workers [6,7] and is defined as the ratio between the (momentary) coverage and the

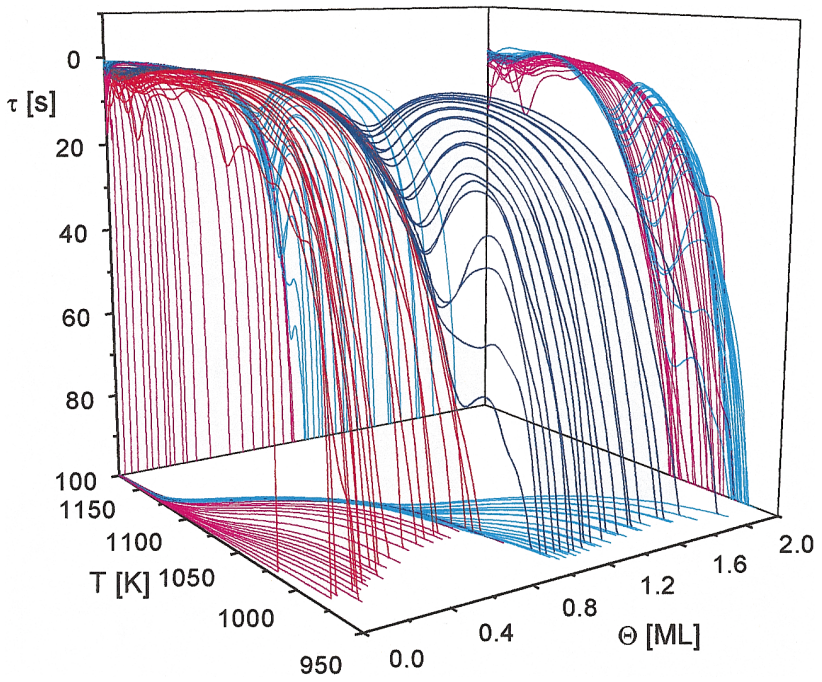

Fig. 6. Three-dimensional graph of the mean lifetime τ as a function of coverage and temperature. Note that the lifetime is plotted inversely (from top to bottom) so that the long-living stable states appear at the bottom of the figure.

rate of change or mass flow (i.e., of desorption):

$$\tau(\Theta, T) = \frac{\Theta_i}{R_i}. \tag{6}$$

In an analogous manner as we treated the desorption rate we can consider also the mean lifetime as a function of the two variables, temperature and coverage, and construct a three-dimensional plot which is shown as Fig. 6. In this graph, we have plotted the lifetime τ from top to bottom; i.e., the low-lying τ values correspond to long-living (favorable) states. According to Eqs. (5) and (6), the mean lifetime depends crucially on the heating rate β. This can also be shown experimentally. We performed TPD measurements with different heating rates and found much shorter lifetimes for higher β values [22]. As before (cf. Fig. 3), we can look at the projections of the function $\tau(\Theta, T)$ on to the temperature or the coverage plane, and we have indicated these projections in Fig. 6. (In the first projection, the parameter is the momentary coverage, in the second one it is the temperature.) We recall that in Bauer's early work on noble metal desorption from tungsten similar diagrams were presented, namely a plot of ln τ versus the coverage Θ, with the temperature functioning as a parameter [6,7].

4. Desorption isotherms and isosters

After the presentation of the principal relations that follow from the Polanyi–Wigner equation it is straightforward to parametrize one of the two independent variables of this equation and evaluate either isothermal (T=constant) or isosteric (Θ=constant) quantities of the desorption reaction. We treated the TPD trajectories of Fig. 3 in just this way. We did this numerically, i.e., we sorted all triples of values $R_{\mathrm{des}}(\Theta, T)$ with respect to the temperature or the coverage, respectively. The result of this procedure is shown in the 3D plot of Fig. 7 and reveals a TPD 'plane' indicated by the area represented by the crossed lines. Within this

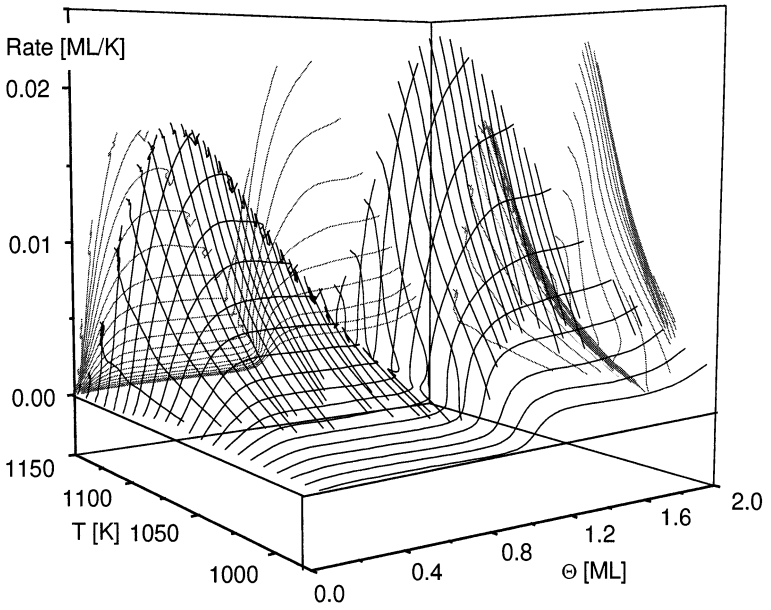

Fig. 7. Parametrized view of the TPD trajectories of Fig. 3. After sorting all triples of values for T, Θ, R_{des} with respect to the temperature or the coverage one obtains a TPD 'plane' which is schematically sketched by a mesh of horizontal and perpendicular lines. Thus, this representation allows us immediately to separate the T, Θ conditions for which a certain desorption kinetics occurs. See text for details.

curved TPD plane we can not only clearly distinguish the first and second monolayer desorption but also recognize local zones which represent areas that increase exponentially with temperature [rate $R(T)$ plane], according to the exponential term in the Polanyi–Wigner equation. On the other hand, we observe horizontal sections of the rate in the $R(\Theta)$ direction. We recall that this behavior is expected if the rate is independent of coverage; hence, it indicates coverage ranges in which the desorption reaction follows a zero-order kinetics. Fig. 7 therefore allows even at first glance to separate just those T, Θ conditions for which zero-order kinetics occurs. Since the zero reaction order is a consequence of a phase equilibrium between 2D condensate and 2D gas phase within the deposit, the respective graph also directly monitors the range of existence of the respective phase equilibrium.

Again, we can also look at the projection of $R_{\mathrm{des}}(\Theta, T)$ in the Θ plane (reproduced as Fig. 8) and identify the horizontal sections as conditions in which zero-order kinetics will be observed,

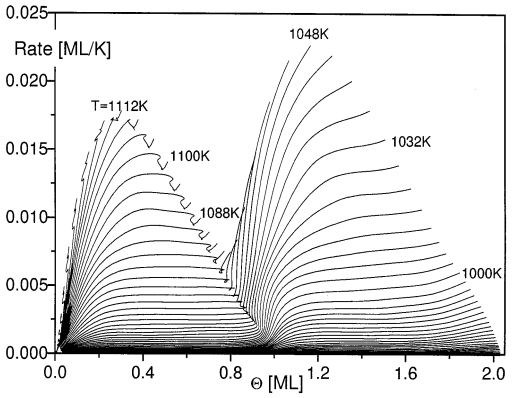

Fig. 8. Projection of the desorption rate $R_{\mathrm{des}}(\Theta, T)$ in the Θ plane, with the temperature T being a parameter. One obtains the so-called desorption isotherms in which horizontal sections indicate a zero-order desorption kinetics.

according to the relation

$$R_{\mathrm{des}}|_{T=\mathrm{const}} = \frac{\nu(\Theta)}{\beta}\,\Theta^{n}\exp\left(-\frac{Q_{\mathrm{des}}(\Theta)}{RT_0}\right). \qquad (7)$$

Note that for $n=0$ and a horizontal inclination of

the respective function, also the other quantities appearing in the Arrhenius plot must be Θ-independent, otherwise no zero slope would result. Since the temperature is the parameter of these curves we can address them as desorption isotherms. Other authors came to quite similar conclusions [27–35].

So far the construction of Figs. 7 and 8 was solely based on a mathematical or numerical evaluation procedure. One could ask here whether it might be possible to measure desorption isotherms directly. The answer is yes, since Paunov and Bauer [29] performed isothermal desorption experiments with the Cu-on-Mo(110) system and Pavlovska et al. for Au/Mo(110) [30] and found good agreement between the data measured directly and those deduced from the TPD spectra in the manner described above. The (not trivial) experimental procedure was such that the sample was kept at a constant temperature (in the range where desorption takes place) and subjected to a flux of copper atoms from an evaporation source. At time $t_0=0$ the flux was turned off and the resulting desorption trace was monitored.

Another quite revealing way to exploit desorption isotherms starts off from their double-logarithmic representation

$$\ln R_{\mathrm{des}}|_{T=\mathrm{const}} = \ln \frac{\nu(\Theta)}{\beta} + n \ln \Theta + \frac{Q_{\mathrm{des}}(\Theta)}{RT_0}. \qquad (8)$$

Obviously, the slope of such a plot yields directly the desorption order, n. This is why plots of $\ln R_{\mathrm{des}}$ versus $\ln \Theta$ are called 'order plots'. An example is given in Fig. 9 for the Cu-on-Re(0001) system, spanning a coverage range from 0 up to $\sim$2 ML. We can distinguish basically four ranges with a common slope. Especially clear and complete is the situation for isotherms referring to lower temperatures. They possess three sections with slope $\sim$zero while in the last section ($\Theta<0.15$) the slope is approximately unity, indicating a first-order desorption process. The other isotherms exhibit a more or less analogous behavior, although the ranges with constant slope become less pronounced with increasing temperature, the reason being that at elevated temperatures more and more TPD states desorb and

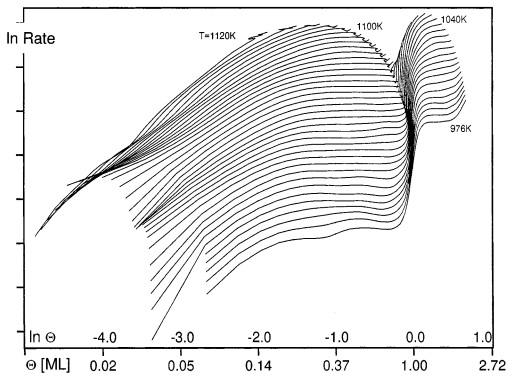

Fig. 9. Double-logarithmic plot of R_{des} versus Θ, according to Eq. (8), for TPD data of the Cu-on-Re(0001) system, spanning a coverage range $0<\Theta<\sim 2$ ML. The slope of this plot yields directly the desorption order, n. This is why these representations are called 'order plots'.

simply disappear from the graph. In our previous paper on copper desorption from Re(0001) [21] we explained the change of the desorption order from one to zero around $\Theta=0.15$ by the existence of a phase equilibrium (due to attractive Cu–Cu interactions) between a 2D copper gas phase and a 2D copper condensed phase (copper islands). (Only for copper coverages $\geq$0.15 ML can the latter phase exist.) For the second copper layer ($\Theta>1$) the same principal features (although somewhat less pronounced) can be distinguished in the order plots. We simply note that Nagai [19] could simulate the same transition from $n=1$ to $n=0$ in his TPD calculations.

If we now consider the projection of $R_{\mathrm{des}}(\Theta, T)$ in the temperature plane (with Θ as a parameter) we obtain desorption isosters (which were already mentioned in the context of Fig. 7). Again, the question arises whether isosters are experimentally accessible, since the desorption process per se is a temperature-induced change of the coverage. One could identify the desorption rate with the flux of particles leaving the sample and reaching the detector (mass filter, etc.). In a Gedankenexperiment, one could then think of providing an artificial flux of exactly the same value back to the sample, in order to compensate the desorptive loss of particles (the isosteric condition must, of course, be maintained). This could principally be achieved by a controlled deposition.

The difficulty is, of course, that the temperature has to be increased in a linear fashion during the individual experimental run — the desorption isosters are seldom presented in the form R_{des} versus $T|_{\Theta\,const}$. If we return to Eq. (8) but write it for isosteric condition it takes the form

$$\ln R_{des}|_{\Theta=const} = \ln \frac{\nu(T)}{\beta} + n \ln \Theta_0 + \frac{Q_{des}(T)}{RT}. \tag{9}$$

We see immediately that a plot of the logarithm of the desorption rate for constant coverage against the reciprocal temperature should yield straight lines whose slope is given by $-Q_{res}/R$ with the intercept $\ln[\nu(T)/\beta] + n \ln \Theta_0$. The respective plot resembles the well-known Arrhenius diagrams appearing in equilibrium thermodynamics or chemical reaction kinetics and revealing (if temperature dependencies are neglected in the range of data evaluation) the desorption energy and (if n is constant) the frequency factor ν. This procedure of Q_{des} evaluation was proposed quite a while ago by King [8]; it is known as complete line-shape analysis. In his article, King also considered the problem of multiple desorption states and overlapping TPD states as well as (coverage-dependent) frequency factors or reaction orders.

At about the same time, a closely related method of determining Q_{des} and ν was suggested by Bauer et al. [6,7] which was also based on the applicability of Eq. (9). However, these authors do not exploit the desorption isosters but rather the lifetime isosters, which can be deduced in an analogous manner from a series of lifetime spectra (cf. Fig. 6) according to the expression:

$$\ln \tau|_{\Theta=const} = -\ln \frac{\nu(T)}{\beta} - (n-1) \ln \Theta_0 - \frac{Q_{des}(T)}{RT}. \tag{10}$$

Principally, there should be and, in fact, there is no difference in the Q_{des} and ν evaluation if the King or the Bauer procedure is applied.

We note that Schlatterbeck et al. used a numerical variant of Bauer's lifetime isoster method to perform a very detailed and precise determination of the coverage dependence of both Q_{des} and ν for the Ag-on-Re(0001) system [36,37]. The aforementioned phase equilibrium between 2D gas and 2D condensed phase exists in quite a similar fashion also for the Ag-on-Re(0001) system, leading to a slight Q_{des} difference for removing a silver atom directly from the 2D condensed phase or from the 2D gas phase (the latter process requires less energy because of the greatly reduced lateral Ag–Ag interactions). Therefore, the existence of the phase equilibrium is reflected in carefully measured isosters by a slight bend in the Arrhenius curves [36].

To give an example also for the Cu-on-Re(0001) system, we present in Fig. 10 a series of Arrhenius-type isosters, evaluated from the graph of Fig. 7. They span the coverage range $0.02 < \Theta < 2$ ML and can be divided into four groups: (1) $0 < \Theta < 0.25$ ML; (2) $0.26 < \Theta < 0.75$ ML; (3) $0.76 < \Theta < 1$ ML; and (4) $\Theta > 1$ ML. Groups (2) and (4) are characterized by a common tail in which they practically fall together, reflecting zero-order kinetics. Groups (1) and (3) behave differently: first the slope of the curves increases slightly when going towards higher coverages, but they still remain essentially linear. However, in group (3) the slope of the isosteres is strongly temperature-dependent, it is steep at lower and flat at higher temperature. It is assumed that coverage- and temperature-dependent phase equilibria affect the behavior of the isosters to a great extent in a

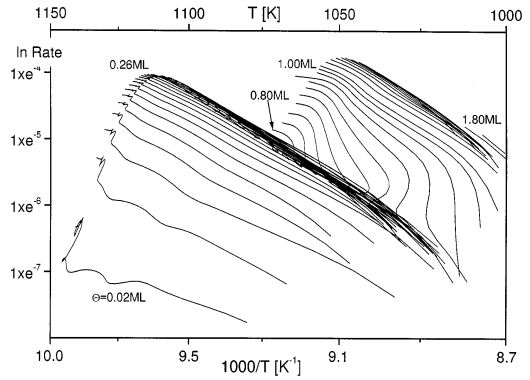

Fig. 10. Series of Arrhenius-type isosters, based on the graph of Fig. 7, again for the Cu-on-Re(0001) system. A total coverage range of $0.02 < \Theta < 2$ ML is monitored which can be subdivided into four groups with different behavior as is explained in more detail in the text.

manner that cannot be predicted precisely. Various reasoning can be invoked to explain this behavior [20,21], namely the existence of non-equivalent adsorption sites [within a single layer (e.g., face-centered cubic and hexagonal close-packed sites) or between the first and second layer], two-dimensional phase equilibria or the fact that pseudomorphic growth phenomena govern the first-layer properties, while the film is relaxed already in the second layer.

5. Conclusions

We have shown in this work that both the rate of a desorption reaction, R_{des}, and the particle lifetime on a surface, τ, must be considered functions of two variables: coverage Θ and temperature T. It is very advantageous to plot these functions as three-dimensional graphs and to illustrate the internal correlation between a 'normal' thermal desorption spectrum, a layer plot, an order plot and desorption isosters. In this way, the numerical determination of characteristic desorption parameters (desorption energy, desorption order, frequency factor, etc.) is greatly facilitated. This could be shown by means of specific examples taken from the system Cu/Re(0001).

Acknowledgements

The present work would not have been possible without financial support by the Deutsche Forschungsgemeinschaft (SFB 290) and vital discussions with D. Schlatterbeck, S.L.M. Schröder and H.J. Kreuzer. We thank R. Cames and K. Schubert for technical support.

References

[1] P.A. Redhead, Vacuum 12 (1962) 203.
[2] G. Carter, Vacuum 12 (1962) 245.
[3] G. Carter, Vacuum 13 (1963) 89.
[4] G. Ehrlich, Adv. Catal. 14 (1963) 255.
[5] L.A. Péterman, Progr. Surf. Sci. 1 (1972) 2.
[6] E. Bauer, H. Poppa, G. Todd, F. Bonczek, J. Appl. Phys. 45 (1974) 5164.
[7] E. Bauer, F. Bonczek, H. Poppa, G. Todd, Surf. Sci. 53 (1975) 87.
[8] D.A. King, Surf. Sci. 47 (1975) 384.
[9] D. Menzel, in: R. Gomer (Ed.), Interactions on Metal Surfaces, Topics in Applied Physics, vol. 4, Springer, Berlin/Heidelberg/New York, 1975, p. 101.
[10] C.M. Chan, R. Aris, W.H. Weinberg, Appl. Surf. Sci. 1 (1978) 360.
[11] C.M. Chan, W.H. Weinberg, Appl. Surf. Sci. 1 (1978) 377.
[12] E. Habenschaden, J. Küppers, Surf. Sci. 138 (1983) L147.
[13] E. Bauer, in: The Chemical Physics of Solid Surfaces and Heterogeneous Catalysis, vol. III, Elsevier, Amsterdam, 1984, p. 1.
[14] A.M. de Jong, J.W. Niemantsverdriet, Surf. Sci. 233 (1991) 355.
[15] H.J. Kreuzer, Surf. Sci. 338 (1995) 261.
[16] S.H. Payne, H.J. Kreuzer, A. Pavlovska, E. Bauer, Surf. Sci. 345 (1996) L1.
[17] S.H. Payne, H.A. MacKay, H.J. Kreuzer, M. Gierer, H. Bludau, H. Over, G. Ertl, Phys. Rev. B 54 (1996) 5073.
[18] V.P. Zhdanov, Surf. Sci. 133 (1983) 469.
[19] K. Nagai, Surf. Sci. 176 (1986) 193.
[20] R. Wagner, Diploma thesis, Free University of Berlin, 1997.
[21] R. Wagner, D. Schlatterbeck, K. Christmann, Surf. Sci. 440 (1999) 231.
[22] R. Wagner, D. Schlatterbeck, K. Christmann, in preparation.
[23] K. Christmann, in: Introduction to Surface Physical Chemistry, Steinkopff-Verlag, Darmstadt, 1991, p. 152 ff.
[24] H. Schlichting, D. Menzel, Surf. Sci. 272 (1992) 27.
[25] M. Head-Gordon, J.C. Tully, H. Schlichting, D. Menzel, J. Chem. Phys. 95 (1991) 9266.
[26] H.J. Kreuzer, Z. Jun, S.H. Payne, W. Nichtl-Pecher, L. Hammer, K. Muller, Surf. Sci. 303 (1994) 1.
[27] H. Pfnür, P. Feulner, H.A. Engelhardt, D. Menzel, Chem. Phys. Lett. 59 (1978) 481.
[28] H. Pfnür, D. Menzel, J. Chem. Phys. 79 (1983) 2400.
[29] M. Paunov, E. Bauer, Appl. Phys. A 44 (1987) 201.
[30] A. Pavlosvka, H. Steffen, E. Bauer, Surf. Sci. 195 (1988) 207.
[31] K. Nagai, A. Hirashima, Surf. Sci. 187 (1987) L616.
[32] H.J. Kreuzer, S.H. Payne, Surf. Sci. 200 (1988) L433.
[33] H.J. Kreuzer, S.H. Payne, Surf. Sci. 205 (1988) 153.
[34] H.J. Kreuzer, Appl. Phys. A 51 (1990) 491.
[35] H.J. Kreuzer, Surf. Sci. 231 (1990) 213.
[36] D. Schlatterbeck, Ph.D. thesis, Freie Universität Berlin, 1998.
[37] D. Schlatterbeck, M. Parschau, K. Christmann, Surf. Sci. 418 (1998) 240.